FEBS Open Bio 4 (2014) 168–174

journal homepage: www.elsevier.com/locate/febsopenbio

Stabilization of cyclohexanone monooxygenase by a computationally designed disulfide bond spanning only one residue

Hugo L. van Beek, Hein J. Wijma, Lucie Fromont, Dick B. Janssen, Marco W. Fraaije *

Department of Biochemistry, Groningen Biomolecular Sciences and Biotechnology Institute, University of Groningen, Nijenborgh 4, 9747 AG Groningen, The Netherlands

ARTICLE INFO

Article history:
Received 10 January 2014
Revised 29 January 2014
Accepted 29 January 2014

Keywords:
Baeyer–Villiger monooxygenase
Computational design
Disulfide bonds
Thermostability
Flavoprotein
Enzyme engineering

ABSTRACT

Enzyme stability is an important parameter in biocatalytic applications, and there is a strong need for efficient methods to generate robust enzymes. We investigated whether stabilizing disulfide bonds can be computationally designed based on a model structure. In our approach, unlike in previous disulfide engineering studies, short bonds spanning only a few residues were included. We used cyclohexanone monooxygenase (CHMO), a Baeyer–Villiger monooxygenase (BVMO) from *Acinetobacter* sp. NCIMB9871 as the target enzyme. This enzyme has been the prototype BVMO for many biocatalytic studies even though it is notoriously labile. After creating a small library of mutant enzymes with introduced cysteine pairs and subsequent screening for improved thermostability, three stabilizing disulfide bonds were identified. The introduced disulfide bonds are all within 12 Å of each other, suggesting this particular region is critical for unfolding. This study shows that stabilizing disulfide bonds do not have to span many residues, as the most stabilizing disulfide bond, L323C–A325C, spans only one residue while it stabilizes the enzyme, as shown by a 6 °C increase in its apparent melting temperature.

1. Introduction

Enzyme stability is an important parameter in biocatalysis, as an increase in stability will improve the economics of enzyme use in industrial applications [1]. Unfortunately most enzymes are relatively unstable, not evolved to operate at high temperatures or in the presence of organic solvents. Improvements in thermostability are often laborious and usually require the creation and screening of large enzyme mutant libraries [2]. In most proteins, stabilizing mutations are found in certain critical regions, suggesting structural regions that allow early unfolding steps of an enzyme, while mutations elsewhere in the protein have a much smaller effect on thermostability [3–5]. Therefore, there is a need for methods to locate such critical regions [6], to allow enzyme engineering efforts to focus and so to reduce the amount of labor required to stabilize an enzyme [7,8].

Recently, we published an improved computational method for disulfide bond design to boost enzyme stability. For limonene epoxide hydrolase, this resulted in identification of 9 stabilizing disulfide bonds out of the 18 that were experimentally tested [9]. The stabilizing disulfide bonds were clustered at a critical region for stability, where also stabilizing point mutations had most effect [9]. This study showed that by introducing computer-designed disulfide bonds, it is possible to locate the critical region for stabilization using relatively few variants. However, this was done for a protein for which an X-ray structure was available and it is not obvious whether such a strategy would work for a protein for which only a homology model is available. Homology models are structurally far less accurate than (high resolution) X-ray structures [10], which could hinder the computational design of stabilizing disulfide bonds and thus a higher fraction of non-stabilized disulfide bonds can be expected.

Introduced disulfide bonds that contribute to protein stability typically involve disulfide bonds that bridge a large number of residues. The use of disulfide bonds spanning only a few residues is a surprisingly unexplored method to stabilize proteins. Disulfide bonds in natural proteins in majority encompass <30 residues, with most bonds spanning ~11 residues [11]. However, in protein stability engineering, short disulfide bonds are avoided, because it is assumed that the obtained stabilization by a disulfide bond is dominated by the number of residues that the disulfide bond spans across [12]. This proposed correlation between the obtained stabilization and the number of spanned residues is however poorly supported by experimental data. Therefore it appeared

Abbreviations: BVMO, Baeyer–Villiger monooxygenase; CHMO, cyclohexanone monooxygenase; DTT, dithiothreitol; MD, molecular dynamics; PAMO, phenylacetone monooxygenase

* Corresponding author. Tel.: +31 50 363 4345; fax: +31 50 363 4165.
E-mail address: m.w.fraaije@rug.nl (M.W. Fraaije).

http://dx.doi.org/10.1016/j.fob.2014.01.009
2211-5463/$36.00

worthwhile to investigate the effect of introducing very short disulfide bonds, which might have been overlooked earlier [13].

In this study, we test whether computational design of disulfide bonds can be used to find a region critical for unfolding and to stabilize a coenzyme-dependent and cofactor-containing enzyme, cyclohexanone monooxygenase from *Acinetobacter* sp. NCIMB9871 (CHMO), of which no crystal structure is available. While our previous successful disulfide design was based on an X-ray structure of the target enzyme, this time we applied our in-house developed computational design protocol on a homology model. An additional modification was the inclusion in the *in silico* design of short disulfide bonds spanning <15 residues.

The target enzyme, CHMO, can be considered as the prototype enzyme for Baeyer–Villiger monooxygenases (BVMOs), an enzyme class that is attracting an ever-increasing interest for being applied in biocatalytic processes [14–20]. CHMO has been studied for its biocatalytic potential in numerous studies which has revealed that it (1) accepts a wide range of aliphatic substrates, (2) is able to perform chemo- and regioselective oxidations, and (3) yields absolute enantioselectivity for many of the tested conversions [19,21]. In the last decade, it has been the subject of several directed evolution and site-directed mutagenesis studies, aiming at altering the substrate specificity or improving the stability [22–25]. Recently this enzyme was used by Codexis as a starting point in a directed evolution approach to improve the enantioselective production of (*S*)-omeprazole, a blockbuster pharmaceutical [26]. So far, CHMO has defied all crystallization attempts which may partly be due to its notoriously poor thermostability [27–29]. Yet, to guide enzyme engineering attempts of CHMO, crystal structures of the homologous phenylacetone monooxygenase (PAMO) are available [30,31], and more recently the structure of the more closely related CHMO from *Rhodococcus* sp. was elucidated [32,33].

Previously we attempted to access CHMO-like activity in a thermostable enzyme by using PAMO from the thermophile *Thermobifida fusca* as a scaffold to introduce activities of related BVMOs [34]. PAMO has an apparent melting temperature (T_m) more than 20 °C higher than CHMO, but only has a limited substrate range [19,35]. We were able to expand the substrate specificity in a PAMO–CHMO chimera, but activity with the preferred substrate of CHMO, cyclohexanone, was not detected.

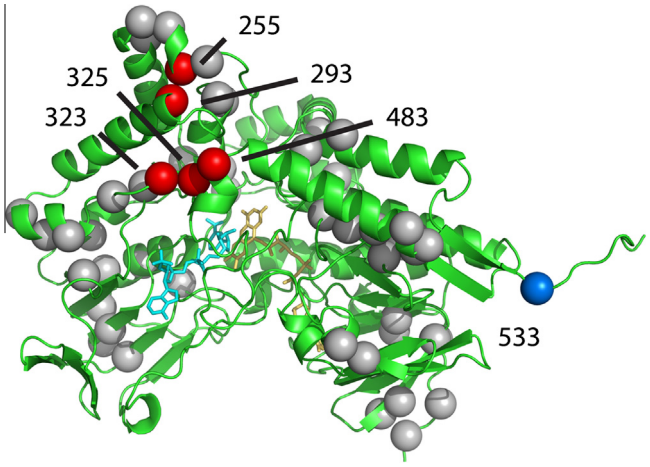

Fig. 1. Model structure of CHMO showing the introduced cysteines as spheres. Non-beneficial mutations are shown in gray, beneficial mutations shown in red. Residues 323–325 are mutated to cysteines in the best mutant, residues 255–293 and 325–483 were mutated in the other two described mutants. Of the truncation mutant, the last C-terminal residue is shown in blue. FAD is shown in yellow; $NADP^+$ is shown in cyan. (For interpretation of the references to color in this figure legend, the reader is referred to the web version of this article.)

Here we report on the introduction of disulfide bonds in CHMO, designed using a homology model based on the X-ray structure of a sequence-related CHMO (58% sequence identity). A total of 27 disulfide bond mutants were designed *in silico* and experimentally tested for their thermostability. Three stabilized mutants were identified, which were all located in the same region. This suggests that this particular region is important for the stabilization of CHMO. The most stabilized disulfide bond variant was L323C–A325C, with an apparent T_m increase of 6 °C and a 12-fold increased half-life, while its disulfide bonds spans only one residue. This illustrates the importance of taking extremely short disulfide bonds into consideration when designing more stable proteins.

2. Results

Disulfide bonds were designed in a model structure of *Acinetobacter* CHMO (see experimental section). To prevent the loss of catalytic activity, no disulfide bonds were allowed between residues that are within 8 Å from the FAD and $NADP^+$ cofactors bound in the homology model. Also, the loop between residues 487–504, which in the *Rhodococcus* CHMO adopts a different conformation in the open and closed form of the enzyme [32], was excluded from mutagenesis. While previously disulfide bonds that spanned <15 residues were not allowed [9], here no such restrictions were implemented. The selected disulfide bonds are distributed over the whole protein, to probe for the regions that are important for thermostability (Fig. 1). Of the 27 selected disulfide bonds, 8 spanned <15 amino acids (Table S1). Additionally, because in the homology model the C-terminal residues 534–545 could not be modeled (absent in the crystal structure), this C-terminus was removed in a separate mutant, as the removal of such disordered C-termini can also increase stability [11].

All mutants were grown in 50 mL TB medium and twenty disulfide bond mutants were expressed and purified in sufficient yield to determine the apparent melting point in the ThermoFAD experiment. In this experiment the enzyme is heated in a RT-PCR machine, and by following the increase in FAD fluorescence when it is released from the protein, the apparent melting point can be determined. Of the twenty purified mutants, three displayed a higher apparent melting temperature than the wild-type CHMO, while for other disulfide bond mutants the apparent melting temperature was similar to the wild-type CHMO or even significantly reduced (Table S1 and Fig. S1). The truncation mutant, missing 10 residues at the C-terminus, was expressed but turned out to be slightly less stable than the wild-type enzyme (Table 1). The best mutant, L323C–A325C, showed a 6 °C increase in apparent melting temperature, while two other mutants, A255C–A293C and A325C–L483C, showed an increase of 2.5 °C (Table 1). For these three mutants the melting curves showed only one maximum, indicating there are no subpopulations in which the disulfide bond is not formed, or formed improperly (Fig. S2).

In addition to the ThermoFAD measurements, enzyme activity was monitored at a single temperature to determine the half-life,

Table 1
Apparent melting temperatures of all studied CHMO variants.

CHMO variant	T_m (°C)
WT	38.0
A255C–A293C	40.5
A325C–L483C	40.5
L323C–A325C	44.0 (36.5)[a]
R534stop	37.0

[a] The melting point for the reduced form, obtained by incubating the enzyme o/n with 1.0 mM DTT.

a more relevant parameter for biocatalysis. For this, incubation at 30 °C was followed by measuring BVMO activity with cyclohexanone as substrate. This revealed that only the L323C–A325C mutant displayed a significantly increased half-life. The time at which 50% catalytic activity was left was increased >10 fold to 45 min for this mutant, compared to 4 min for the wild-type enzyme (Fig. 2). The other two enzymes show inactivation behavior similar to the wild-type enzyme (Fig. S8).

To create an even more stable CHMO mutant, beneficial double mutations were combined. Because the A325C mutation is present in two of the stabilized variants, only two double disulfide bond mutants could be created. Combining A325C–L483C or L323C–A325C with A255C–A293C resulted in two separate melting points in de ThermoFAD experiment (Fig. S3). One subpopulation exhibited a slightly increased apparent melting temperature compared to the single A255C–A293C mutant for both mutants containing two disulfide bonds. Unfortunately a large fraction of the enzyme was less stable. Expression levels of the double mutants were also significantly reduced, probably due to misfolding events as result of the four introduced cysteines.

The L323C–A325C mutant was further investigated as it was the only mutant showing increased stability in both the ThermoFAD experiment and the inactivation assay. In the design process, a minimum distance from the active site was set to prevent mutations close to the active site from influencing the catalytic efficiency or enantioselectivity of the enzyme. To check whether the mutant was an effective enzyme, steady state kinetic parameters were determined (Table 2). While the activity of the mutant was found to be slightly lower than that of the wild-type enzyme, affinities for both cyclohexanone and bicyclo[3.2.0]hept-2-en-6-one are increased. It is worth noting that the activities of the wild-type CHMO and the mutant on the nonphysiological substrate bicyclo[3.2.0]hept-2-en-6-one are almost as high as with cyclohexanone, the natural substrate. For both bicyclo[3.2.0]hept-2-en-6-one and thioanisole the products are formed with complete enantioselectivity for the wild-type and mutant enzymes. These results show that introduction of the two cysteines yields a catalytically competent enzyme. From the apparent half-life and the k_{cat}, the TTN (total turnover number) was calculated [36]. The TTN for the mutant enzyme (24×10^3) is 5-fold higher than the TTN for the wild-type enzyme (4.5×10^3).

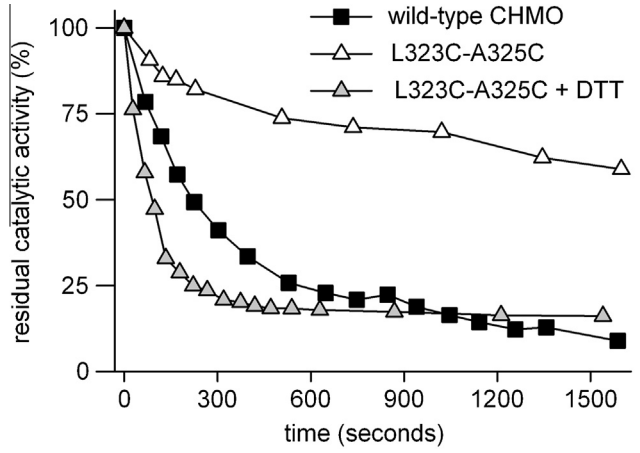

Fig. 2. Enhanced stability of CHMO by an introduced disulfide bond. Enzyme was incubated at 30 °C in the presence of 0.5 mM cyclohexanone and activity was measured at different time points. The relative initial rates after addition of 100 μM NADPH are plotted with the activity at $t = 0$ set to 100%. The L323C–A325C mutant (open triangles), wild-type (squares) and the reduced L323C–A325C mutant (grey triangles) are shown here, see Fig. S8 for an extended graph also including data for the other two single disulfide bond mutants.

The lowered activity of the mutant could be recovered after incubation with a reducing agent (DTT); after incubation the observed rate increased with 54% (9.4 s^{-1} vs. 6.1 s^{-1}). This indicates that the reduced activity is caused by the formation of a disulfide bond as opposed to the effect of the introduction of two separate cysteine thiols. The addition of DTT has some inhibitory effect on the enzyme activity (Fig. S4), but this is insignificant at the residual concentration (20 μM) in this experiment.

Because the release of $NADP^+$ is the rate-limiting step in the catalytic cycle of CHMO, a change in the binding or release of $NADP^+$ directly affects the steady state behavior of the enzyme [37]. The microenvironment of FAD changes upon binding of $NADP^+$, resulting in a reduced absorbance, with a maximum decrease at 387 nm. By observing this change in the spectrum of FAD, the affinity for $NADP^+$ could be determined. The K_D for $NADP^+$ was significantly decreased to 15 μM for the L323C–A325C mutant compared to a K_D of 28 μM for the wild-type enzyme (Table S2 and Fig. S6). Upon reduction of the enzyme, the K_D for $NADP^+$ is increased to 46 μM, significantly above the value for the wild-type enzyme. This agrees with the effects on the observed rates, suggesting that the formation of the disulfide bond affects the k_{cat} *via* a change in $NADP^+$ affinity.

The reduction of the L323C–A325C disulfide bond was further investigated by observing the spectroscopic properties of FAD. During incubation with DTT the spectrum changes and the secondary absorbance maximum of the L323C–A325C enzyme at 369 nm moves to the wild-type value of 380 nm (Fig. S5). In the ThermoFAD assay, we observe that incubation with DTT reduces the stability of the L323C–A325 mutant by 7.5 °C, making the reduced enzyme more unstable than the wild-type CHMO (Table 1 and Fig. S2). This experiment also shows that the reduction of the L323C–A325C mutant is complete, as there is no residual subpopulation with a higher apparent melting temperature. Finally, also in the time-dependent inactivation experiment the stability of the reduced L323C–A325C mutant is dramatically reduced (Fig. 2).

3. Discussion

Stabilizing disulfide bonds were designed and selected *in silico*, based on the model structure of CHMO. Of the 27 mutants containing two additional cysteines that were created, 20 mutants could be expressed and purified. Of this set of mutants, three had a significantly higher apparent melting temperature compared to the wild-type enzyme. The three stabilizing disulfide bonds are located in the same region (Fig. 1), which indicates that this region is important for thermostability. Thus, it appears to be possible to locate a critical region for protein thermostability by testing a series of disulfide bonds that are spread over the protein. While the

Table 2
Steady-state kinetic parameters of the studied enzyme variants. Standard errors for k_{cat} values are <5%, for K_M values <25%. Exact errors are reported in Table S3.

Enzyme	Cyclohexanone		Bicyclo[3.2.0]hept-2-en-6-one		NADPH	
	k_{cat} (s^{-1})	K_M (μM)	k_{cat} (s^{-1})	K_M (μM)	K_M (μM)	Uncoupling rate (s^{-1})
WT-CHMO	14.2	3.6	13.4	1.3	16	0.2
L323C–A325C	6.1	3.0	4.9	0.7	13	0.2

model structure was used successfully to create disulfide bonds, it cannot be investigated whether additional stabilizing disulfide bonds would have been obtained if a high-resolution X-ray structure had been available. On the other hand the success of this method makes it a viable approach to design structurally guided mutants for an enzyme for which no structure is available.

While three of the mutants show a higher apparent melting point in the ThermoFAD method, only the L323C–A325C mutant also showed a significantly extended lifetime in the time-dependent inactivation experiment. Higher apparent melting temperatures often correlate with an increased half-life at a single temperature, but this does not always need to be the case, as during high temperature melting a different mechanism can occur than during low temperature inactivation [38–40]. Regardless of the cause of these differences, the mutant with the longest half-life, L323C–A325C, could be easily identified by the ThermoFAD assay, confirming its potential as a powerful and simple initial screening method [41].

The L323C–A325C mutant was investigated in more detail. The disulfide bond lowers the catalytic activity to some extent, but taken together with the increased stability its TTN was significantly increased (5-fold). This is an important parameter, as it can be used directly to calculate the economic feasibility of a biocatalytic process. Furthermore, enantioselectivities with bicyclo[3.2.0]hept-2-en-6-one and thioanisole were preserved, and affinities for the tested (co)substrates were similar. This shows that by preserving the residues close to the active site and both cofactors, the actual substrate binding site is not altered. Only the activity of the enzyme is slightly reduced.

This activity-reducing effect could be cured by reduction of the disulfide bond, indicating the formation of the bond is the cause for this change in behavior. The disulfide bond is close to residues 324–328, which shift on average 1.7 Å between the open and closed conformations in CHMO [32]. Furthermore, two conserved residues important for catalysis, K326 and R327, are located directly next to the introduced disulfide bond (Fig. 3). K326 binds the phosphate of NADPH and is therefore important for the preference towards NADPH over NADH [42,43]. R327 moves 2.7 Å between the two crystallized CHMO conformations, forming a hydrogen bond with $NADP^+$ [32]. The bound $NADP^+$ has been shown to have a role in stabilizing the peroxyflavin intermediate [44] and detailed kinetic analysis of CHMO has revealed that the release of $NADP^+$ is limiting the rate of catalysis [37]. This indicates that effects on the binding or release of the coenzyme will directly translate into effects on the steady-state kinetic behavior. The introduction of the disulfide bond was indeed found to influence the binding constant of the nicotinamide cofactor which is in line with a lowered k_{cat}. Possibly by altering the exact conformation of the neighboring residues K326 and R327, the disulfide bond had a modest but significant kinetic effect even though the cysteines are more than 8 Å away from both cofactors (Fig. 3).

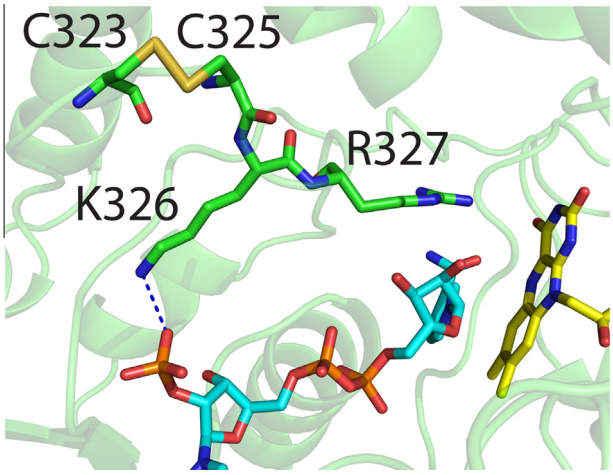

Fig. 3. Modeled structure of the 323–325 disulfide bond, K326 and R327. The interaction of K326 with the phosphate moiety of the $NADP^+$ coenzyme is marked by the dashed line. The FAD prosthetic group is shown in yellow; the $NADP^+$ coenzyme is shown in cyan. (For interpretation of the references to color in this figure legend, the reader is referred to the web version of this article.)

The observation in this study that the most stabilizing engineered disulfide bond only spans one residue seems odd in light of the classical explanation of protein stabilization by disulfide bonds. The common explanation [45] is that the disulfide bond primarily stabilizes a protein by lowering the entropy of the unfolded state. With this explanation it can be derived that a protein should be stabilized by a disulfide bond according to [13,46]:

$$\Delta S \approx -1.5\,R\ln(N) \quad (1)$$

In which N is the number of residues spanned by the disulfide bond and R is the gas constant. While this equation was devised for reversible folding, it is normally assumed that reversible unfolding precedes irreversible protein inactivation. Thus the trends predicted by the above equation, a stronger stabilization at higher N, should also hold for irreversible processes.

However, it has been argued that this explanation should be abandoned and that Eq. (1) has no predictive value [13,47]. Experimental results as reviewed by [13] reveal no correlation between the number of residues that disulfide bonds encompass and their stabilizing effect. This lack of correlation is also supported by our data (Table S1 and Fig. S1), in which a disulfide bond that stretches over 157 residues was less stabilizing than a disulfide bridge that extended across only 1 residue. Other existing arguments against the validity of Eq. (1) are that its derivation assumes a random coil in the unfolded state [13], which has been shown to be an oversimplification, and that enthalpic contributions of disulfide bonds to stability are five times larger than entropic contributions [47]. Nature prefers disulfide bonds to stretch over relative few residues, most commonly approximately 11 residues [11,13,48] while Eq. (1) predicts it should be far more favorable for protein stability to maximize the number of residues in the disulfide loop [46]. An alternative explanation for the stabilizing effects of disulfide bonds is that mainly local interactions introduced by the disulfide bond stabilize the protein [13]. Thus, since the classical explanation for how disulfide bonds stabilize proteins may very well be wrong, we see no reason to avoid disulfide bonds that stretch over only a few residues. The results obtained here with a disulfide bond that only spans one residue demonstrate that such disulfide bonds encompassing only a few residues can indeed be of use for stabilizing a protein.

4. Materials and methods

4.1. Materials

DpnI was acquired from New England Biolabs, $NADP^+$ and NADPH from Oriental Yeast Co., Ni-Sepharose from GE-healthcare and all other chemicals were from Sigma–Aldrich. Oligonucleotides were synthesized by Eurofins MWG Operon and Sigma–Aldrich. Sequencing to confirm plasmid sequences was done at GATC-biotech.

4.2. Homology modeling

A homology model was constructed using YASARA [10,49,50]. The homology model was based on the 2.3 Å resolution X-ray structure of a *Rhodococcus* sp. CHMO in its closed form, with FAD and NADPH bound (PDB: 3GWD) [32]. Of the 543 residues from

Acinetobacter CHMO, 527 (97%) could be aligned to 3GWD with 58% sequence identity and 75% sequence similarity. After inspection of an initial model, 33 water molecules of 3GWD were deleted that appeared to be incompatible with the structure of the modeled *Acinetobacter* CHMO. The remaining 116 water molecules, often making H-bonds between backbones and conserved side-chains, were preserved. The resulting model was scored under YASARA and qualified as "good" with a Z-score of −0.44.

4.3. Design of disulfide bond mutants

Disulfide bonds were designed by the Disulfide Discovery protocol as described earlier with identical geometric and energetic criteria [9]. The procedure uses MD simulations to sample the backbone structural flexibility. The protocol for these MD simulations was described earlier [51]. These MD simulations of the modeled structure consisted of 5 trajectories that were started with different initial velocities [52] to obtain independent trajectories. After using 30 ps to gradually increase the temperature of the simulation from 5 to 298 K, snapshots of the simulation were recorded at 750 ps, 1500 ps, 2250 ps, and 3000 ps. These snapshots were used to search for positions where a disulfide bond could be introduced that falls within the range of geometries observed for natural disulfide bonds [11]. Subsequently, an *in silico* screening is used to eliminate disulfide bonds that are unlikely to stabilize the structure because they introduce clearly destabilizing features. On the resulting structures with disulfide bonds a second round of MD simulations is carried out [9]. This is done to eliminate variants that increase local flexibility, which is expected to decrease stability [53]. In the first round 57 disulfide bounds were designed of which 30 were eliminated using MD simulations [53]. All disulfide bonds that were generated by the design procedure and passed these earlier described *in silico* screening steps [9] were characterized experimentally.

4.4. Site-directed mutagenesis

After 27 mutants were selected to be tested *in vitro*, the Agilent primer design tool (www.agilent.com) was used to design the primers to create these mutants using QuikChange site-directed mutagenesis. Some modifications were made on the output of this tool, as mutations close to other mutations gave overlapping primers. In those cases, both primers were combined into one long primer without further adaptations. Oligonucleotide sequences are available upon request. 2 or 4 primers were used in each PCR reaction, using the PfuUltra II Master Mix (Agilent) as recommended by the supplier. Primers were ordered as 100 μM stock solutions and combined (4 or 2 primers) to a final concentration of 10 μM. The pCRE2-CHMO construct was used as a template which results in expression of CHMO N-terminally fused to a His-tagged phosphite dehydrogenase that facilitates cofactor regeneration and Ni-affinity purification [54]. PCR reactions, digestions with DpnI and transformations to *E. coli* TOP10 (Invitrogen) were performed in 96-well plates. Because single mutants are sometimes created using this PCR-based method, 4 clones per reaction were sent for sequencing ensuring at least one mutant containing both mutations. Mutants containing combinations of beneficial disulfide bonds were created in the same manner, using adapted primers where needed to prevent reversions to wild-type residues.

4.5. Growth and purification

For each mutant 0.5 mL LB-Amp in a deep-well microtiter plate was inoculated from a glycerol stock and grown overnight at 37 °C. 50 mL TB-Amp was inoculated with this culture and grown at 24 °C for 2 h. 0.02% (w/v) L-Arabinose was added to induce enzyme production for 22 h at 24 °C. The culture was pelleted and resuspended in 5 mL of 50 mM Tris–HCl, pH 7.5 supplemented with 10 μM FAD. Cells were lysed by sonication and cell debris was removed by centrifugation. The resulting cell-free extract was applied on 200 μL of Ni-Sepharose and incubated for 1 h at 4 °C. The column material was separated from the cell-free extract, washed with 3 column volumes of 50 mM Tris–HCl, pH 7.5 and subsequently with 3 column volumes of 50 mM Tris–HCl, pH 7.5 with 5.0 mM imidazole. The enzyme was eluted using 50 mM Tris–HCl pH 7.5 containing 500 mM imidazole. For smaller purifications, the enzyme was concentrated and diluted to reduce the imidazole concentration to 0.5 mM using an Amicon Ultra® Centrifugal Filter. Larger scale purifications were done with selected enzymes, in those cases a Bio-Rad 10DG desalting column was used to remove imidazole. Absorbance at 440 nm was used to determine the concentration of the purified enzyme, using 13.8 mM^{-1} cm^{-1} as the extinction coefficient [37].

4.6. Activity measurements and kinetics

Activities were determined using 100 μM NADPH, 0.05 μM enzyme and 0.5 mM cyclohexanone in 50 mM Tris–HCl pH 8.5 at 20 °C. The absorbance decrease at 340 nm was measured to determine the initial rate. Concentrations of substrates were changed to allow the determination of the different steady-state kinetic parameters. The pH of the Tris–HCl buffer was varied between 7.0 and 9.4 to determine the pH optimum. Because of the high affinity for the substrates, several K_M values were measured using depletion curves, calculating the rate and concentration at every point in a reaction going to completion. For the chemically reduced enzymes, the reported k_{cat} is the rate measured at a saturating concentration (0.5 mM) of cyclohexanone.

4.7. Stability assays

Inactivation of the enzyme was measured by incubating a solution containing 0.05 μM of enzyme, 100 μM $NADP^+$, 0.5 mM cyclohexanone in 50 mM Tris–HCl pH 8.5 at 30 °C. Samples were taken at different time points and activity was measured at 30 °C after addition of NADPH (100 μM).

4.8. Reduction of the enzyme

Reduction of the disulfide bonds was done with 10 mM DTT (dithiothreitol) at room temperature, and spectra were collected every 3 min to follow the reduction. For further experiments, the enzyme was reduced o/n on ice using 1.0 mM DTT.

4.9. ThermoFAD

The ThermoFAD method [41] was used to determine the apparent melting points of the different enzyme variants. Using an RT-PCR machine (CFX96-Touch, Bio-Rad) the fluorescence of the FAD cofactor was monitored using a 450–490 excitation filter and a 515–530 nm emission filter, typically used for SYBR Green based RT-PCR. The temperature was increased with 0.5 °C per step, starting at 25 °C and ending at 90 °C, using a 10 s holding time at each step. The maximum of the first derivative of the observed flavin fluorescence was taken as the apparent melting temperature.

4.10. Conversions

Reactions with bicyclo[3.2.0]hept-2-en-6-one and thioanisole were set up to determine the enantioselectivity of the mutant enzymes. For this, 1.0 mL of 4.0 μM enzyme, 8.0 μM additional PTDH, 10 mM substrate (thioanisole or bicyclo[3.2.0] hept-2-en-6-one),

25 mM phosphite and 100 μM NADPH in 50 mM Tris–HCl pH 8.5 was incubated for 16 h at 30 °C. Samples were extracted with ethyl acetate containing 0.01% (v/v) mesitylene, dried over $MgSO_4$ and analyzed by GC (Chiraldex GT-A column), using separation protocols as described before [35].

Funding information

This work was supported by the EU seventh framework programe (FP7), the Oxygreen project, contract no. 212281. HJW was supported by NWO (Netherlands Organization for Scientific Research) through an ECHO grant.

Appendix A. Supplementary data

Supplementary data associated with this article can be found, in the online version, at http://dx.doi.org/10.1016/j.fob.2014.01.009.

References

[1] Bornscheuer, U., Huisman, G., Kazlauskas, R., Lutz, S., Moore, J. and Robins, K. (2012) Engineering the third wave of biocatalysis. Nature 485, 185–194.
[2] Bommarius, A.S., Broering, J.M., Chaparro-Riggers, J.F. and Polizzi, K.M. (2006) High-throughput screening for enhanced protein stability. Curr. Opin. Biotechnol. 17, 606.
[3] Eijsink, V.G.H., Bjørk, A., Gåseidnes, S., Sirevåg, R., Synstad, B., Burg, B. and Vriend, G. (2004) Rational engineering of enzyme stability. J. Biotechnol. 113, 105–120.
[4] Van den Burg, B., Vriend, G., Veltman, O.R., Venema, G. and Eijsink, V.G. (1998) Engineering an enzyme to resist boiling. Proc. Natl. Acad. Sci. U.S.A. 95, 2056–2060.
[5] Eijsink, V.G., Vriend, G., van der Vinne, B., Hazes, B., van den Burg, B. and Venema, G. (1992) Effects of changing the interaction between subdomains on the thermostability of Bacillus neutral proteases. Proteins 14, 224–236.
[6] Wijma, H.J., Floor, R.J. and Janssen, D.B. (2013) Structure-and sequence-analysis inspired engineering of proteins for enhanced thermostability. Curr. Opin. Struct. Biol. 23, 588–594.
[7] Reetz, M.T. and Carballeira, J.D. (2007) Iterative saturation mutagenesis (ISM) for rapid directed evolution of functional enzymes. Nat. Protoc. 2, 891–903.
[8] Jochens, H., Aerts, D. and Bornscheuer, U.T. (2010) Thermostabilization of an esterase by alignment-guided focussed directed evolution. Protein Eng. Des. Sel. 23, 903–909.
[9] Wijma, H.J., Floor, R. and Janssen, D.B. (2014) Computationally designed libraries for rapid enzyme stabilization. Protein Eng. Des. Sel. 27, 49–58.
[10] Krieger, E., Joo, K., Lee, J., Lee, J., Raman, S., Thompson, J., Tyka, M., Baker, D. and Karplus, K. (2009) Improving physical realism, stereochemistry, and side-chain accuracy in homology modeling: four approaches that performed well in CASP8. Proteins 77, 114–122.
[11] Petersen, M.T.N., Jonson, P.H. and Petersen, S.B. (1999) Amino acid neighbours and detailed conformational analysis of cysteines in proteins. Protein Eng. 12, 535–548.
[12] Dombkowski, A.A., Sultana, K.Z. and Craig, D.B. (2013) Protein disulfide engineering. FEBS Lett. 588, 206–212.
[13] Betz, S.F. (2008) Disulfide bonds and the stability of globular proteins. Protein Sci. 2, 1551–1558.
[14] Chen, Y., Peoples, O. and Walsh, C. (1988) *Acinetobacter* cyclohexanone monooxygenase: gene cloning and sequence determination. J. Bacteriol. 170, 781–789.
[15] Ryerson, C.C., Ballou, D.P. and Walsh, C. (1982) Mechanistic studies on cyclohexanone oxygenase. Biochemistry 21, 2644–2655.
[16] Donoghue, N.A., Norris, D.B. and Trudgill, P.W. (1976) The purification and properties of cyclohexanone oxygenase from *Nocardia globerula* CL1 and *Acinetobacter* NCIB 9871. Eur. J. Biochem. 63, 175–192.
[17] de Gonzalo, G., Mihovilovic, M.D. and Fraaije, M.W. (2010) Recent developments in the application of Baeyer–Villiger monooxygenases as biocatalysts. Chembiochem 11, 2208–2231.
[18] Torres Pazmiño, D.E., Dudek, H.M. and Fraaije, M.W. (2010) Baeyer–Villiger monooxygenases: recent advances and future challenges. Curr. Opin. Chem. Biol. 14, 138–144.
[19] Leisch, H., Morley, K. and Lau, P.C.K. (2011) Baeyer–Villiger monooxygenases: more than just green chemistry. Chem. Rev. 111, 4165–4222.
[20] Kadow, M., Loschinski, K., Mallin, H., Saß, S. and Bornscheuer, U. (2012) Discovery, application and protein engineering of Baeyer–Villiger monooxygenases for organic synthesis. Org. Biomol. Chem. 10, 6249–6265.
[21] Fink, M.J., Rial, D.V., Kapitanova, P., Lengar, A., Rehdorf, J., Cheng, Q., Rudroff, F. and Mihovilovic, M.D. (2012) Quantitative comparison of chiral catalysts selectivity and performance. A generic concept illustrated with cyclododecanone monooxygenase as Baeyer–Villiger biocatalyst. Adv. Synth. Catal. 354, 3491–3500.
[22] Mihovilovic, M.D., Rudroff, F., Winninger, A., Schneider, T., Schulz, F. and Reetz, M.T. (2006) Microbial Baeyer–Villiger oxidation: stereopreference and substrate acceptance of cyclohexanone monooxygenase mutants prepared by directed evolution. Org. Lett. 8, 1221–1224.
[23] Opperman, D.J. and Reetz, M.T. (2010) Towards practical Baeyer–Villiger monooxygenases: design of cyclohexanone monooxygenase mutants with enhanced oxidative stability. Chembiochem 11, 2589–2596.
[24] Reetz, M.T., Brunner, B., Schneider, T., Schulz, F., Clouthier, C.M. and Kayser, M.M. (2004) Directed evolution as a method to create enantioselective cyclohexanone monooxygenases for catalysis in Baeyer–Villiger reactions. Angew. Chem. Int. Ed. 43, 4075–4078.
[25] Reetz, M.T., Daligault, F., Brunner, B., Hinrichs, H. and Deege, A. (2004) Directed evolution of cyclohexanone monooxygenases: enantioselective biocatalysts for the oxidation of prochiral thioethers. Angew. Chem. Int. Ed. 43, 4078–4081.
[26] Y.K.,Bong, M.D., Clay, S.J., Collier, B., Mijts, M., Vogel, X., Zhang, J., Zhu, J., Nazor, D., Smith, S., Song. Synthesis of prazole compounds, European Patent Application No. EP2010836590, 2013.
[27] Secundo, F., Zambianchi, F., Crippa, G., Carrea, G. and Tedeschi, G. (2005) Comparative study of the properties of wild type and recombinant cyclohexanone monooxygenase, an enzyme of synthetic interest. J. Mol. Catal. B 34, 1–6.
[28] Zambianchi, F., Pasta, P., Carrea, G., Colonna, S., Gaggero, N. and Woodley, J.M. (2002) Use of isolated cyclohexanone monooxygenase from recombinant *Escherichia coli* as a biocatalyst for Baeyer–Villiger and sulfide oxidations. Biotechnol. Bioeng. 78, 489–496.
[29] Staudt, S., Bornscheuer, U.T., Menyes, U., Hummel, W. and Gröger, H. (2013) Direct biocatalytic one-pot-transformation of cyclohexanol with molecular oxygen into ε-caprolactone. Enzyme Microb. Technol. 53, 288–292.
[30] Malito, E., Alfieri, A., Fraaije, M.W. and Mattevi, A. (2004) Crystal structure of a Baeyer–Villiger monooxygenase. Proc. Natl. Acad. Sci. U.S.A. 101, 13157–13162.
[31] Orru, R., Dudek, H.M., Martinoli, C., Torres Pazmiño, D.E., Royant, A., Weik, M., Fraaije, M.W. and Mattevi, A. (2011) Snapshots of enzymatic Baeyer–Villiger catalysis: oxygen activation and intermediate stabilization. J. Biol. Chem. 286, 29284–29291.
[32] Mirza, I.A., Yachnin, B.J., Wang, S., Grosse, S., Bergeron, H., Imura, A., Iwaki, H., Hasegawa, Y., Lau, P.C. and Berghuis, A.M. (2009) Crystal structures of cyclohexanone monooxygenase reveal complex domain movements and a sliding cofactor. J. Am. Chem. Soc. 131, 8848–8854.
[33] Yachnin, B.J., Sprules, T., McEvoy, M.B., Lau, P.C. and Berghuis, A.M. (2012) The substrate-bound crystal structure of a Baeyer–Villiger monooxygenase exhibits a Criegee-like conformation. J. Am. Chem. Soc. 134, 7788.
[34] Fraaije, M.W., Wu, J., Heuts, D.P., van Hellemond, E.W., Spelberg, J.H. and Janssen, D.B. (2005) Discovery of a thermostable Baeyer–Villiger monooxygenase by genome mining. Appl. Microbiol. Biotechnol. 66, 393–400.
[35] van Beek, H.L., de Gonzalo, G. and Fraaije, M.W. (2012) Blending Baeyer–Villiger monooxygenases: using a robust BVMO as a scaffold for creating chimeric enzymes with novel catalytic properties. Chem. Commun. 48, 3288–3290.
[36] Rogers, T.A. and Bommarius, A.S. (2010) Utilizing simple biochemical measurements to predict lifetime output of biocatalysts in continuous isothermal processes. Chem. Eng. Sci. 65, 2118–2124.
[37] Sheng, D., Ballou, D.P. and Massey, V. (2001) Mechanistic studies of cyclohexanone monooxygenase: chemical properties of intermediates involved in catalysis. Biochemistry 40, 11156–11167.
[38] Korkegian, A., Black, M.E., Baker, D. and Stoddard, B.L. (2005) Computational thermostabilization of an enzyme. Science 308, 857–860.
[39] Joo, J.C., Pohkrel, S., Pack, S.P. and Yoo, Y.J. (2010) Thermostabilization of *Bacillus circulans* xylanase via computational design of a flexible surface cavity. J. Biotechnol. 146, 31–39.
[40] Joo, J.C., Pack, S.P., Kim, Y.H. and Yoo, Y.J. (2011) Thermostabilization of *Bacillus circulans* xylanase: computational optimization of unstable residues based on thermal fluctuation analysis. J. Biotechnol. 151, 56–65.
[41] Forneris, F., Orru, R., Bonivento, D., Chiarelli, L.R. and Mattevi, A. (2009) ThermoFAD, a Thermofluor®-adapted flavin ad hoc detection system for protein folding and ligand binding. FEBS J. 276, 2833–2840.
[42] Kamerbeek, N.M., Fraaije, M.W. and Janssen, D.B. (2004) Identifying determinants of NADPH specificity in Baeyer–Villiger monooxygenases. Eur. J. Biochem. 271, 2107–2116.
[43] Dudek, H.M., Torres Pazmiño, D.E., Rodríguez, C., de Gonzalo, G., Gotor, V. and Fraaije, M.W. (2010) Investigating the coenzyme specificity of phenylacetone monooxygenase from Thermobifida fusca. Appl. Microbiol. Biotechnol. 88, 1135–1143.
[44] Torres Pazmiño, D.E., Baas, B.J., Janssen, D.B. and Fraaije, M.W. (2008) Kinetic mechanism of phenylacetone monooxygenase from *Thermobifida fusca*. Biochemistry 47, 4082–4093.
[45] Fersht, A. (1999) Structure and Mechanism in Protein Science, 2nd edition, WH Freeman & Co, New York.
[46] Matsumura, M., Becktel, W.J., Levitt, M. and Matthews, B.W. (1989) Stabilization of phage T4 lysozyme by engineered disulfide bonds. Proc. Natl. Acad. Sci. U.S.A. 86, 6562–6566.
[47] Doig, A.J. and Williams, D.H. (1991) Is the hydrophobic effect stabilizing or destabilizing in proteins? The contribution of disulphide bonds to protein stability. J. Mol. Biol. 217, 389.

[48] Thornton, J. (1981) Disulphide bridges in globular proteins. J. Mol. Biol. 151, 261–287.
[49] Mückstein, U., Hofacker, I.L. and Stadler, P.F. (2002) Stochastic pairwise alignments. Bioinformatics 18, S153–S160.
[50] Canutescu, A.A. and Dunbrack, R.L. (2009) Cyclic coordinate descent: a robotics algorithm for protein loop closure. Protein Sci. 12, 963–972.
[51] Westerbeek, A., Szymański, W., Wijma, H.J., Marrink, S.J., Feringa, B.L. and Janssen, D.B. (2011) Kinetic resolution of α-bromoamides: experimental and theoretical investigation of highly enantioselective reactions catalyzed by haloalkane dehalogenases. Adv. Synth. Catal. 353, 931–944.
[52] Caves, L.S.D., Evanseck, J.D. and Karplus, M. (1998) Locally accessible conformations of proteins: multiple molecular dynamics simulations of crambin. Protein Sci. 7, 649–666.
[53] Vihinen, M. (1987) Relationship of protein flexibility to thermostability. Protein Eng. 1, 477–480.
[54] Torres Pazmiño, D.E., Riebel, A., de Lange, J., Rudroff, F., Mihovilovic, M.D. and Fraaije, M.W. (2009) Efficient biooxidations catalyzed by a new generation of self-sufficient Baeyer–Villiger monooxygenases. Chembiochem 10, 2595–2598.